ADVANCES IN ATMOSPHERIC SCIENCES, VOL. 20, NO. 5, 2003, PP. 743–754

Regime Shifts in the North Pacific Simulated by a COADS-driven Isopycnal Model

WANG Dongxiao*[1,2] (王东晓), WANG Jia[3] (王 佳), Lixin WU[4] (吴立新), and Zhengyu LIU[4] (刘征宇)

[1] *LED, South China Sea Institute of Oceanology, Chinese Academy of Sciences, Guangzhou* 510301

[2] *Guangzhou Institute of Tropical Ocean and Meteorology, CMA, Guangzhou* 510080

[3] *International Arctic Research Center, University of Alaska Fairbanks, Alaska* 99775-7340, *USA*

[4] *Department of Atmospheric and Oceanic Sciences, University of Wisconsin-Madison, Wisconsin* 53706-1695, *USA*

(Received 30 August 2002; revised 22 January 2003)

ABSTRACT

The Miami Isopycnal Coordinate Ocean Model (MICOM) is adopted to simulate the interdecadal variability in the Pacific Ocean with most emphasis on regime shifts in the North Pacific. The computational domain covers 60°N to 40°S with an enclosed boundary condition for momentum flux, whereas there are thermohaline fluxes across the southern end as a restoring term. In addition, sea surface salinity of the model relaxes to the climatological season cycle, which results in climatological fresh water fluxes. Surface forcing functions from January 1945 through December 1993 are derived from the Comprehensive Ocean and Atmospheric Data Set (COADS). Such a numerical experiment reproduces the observed evolution of the interdecadal variability in the heat content over the upper 400-m layer by a two-year lag. Subduction that occurs at the ventilated thermocline in the central North Pacific is also been simulated and the subducted signals propagate from 35°N to 25°N, taking about 8 to 10 years, in agreement with the eXpendable Bathy Thermograph observation over recent decades. Interdecadal signals take a southwestward and downward path rather than westward propagation, meaning they are less associated with the baroclinic planetary waves. During travel, the signals appear to conserve potential vorticity. Therefore, the ventilated thermocline and related subduction are probably the fundamental physics for interdecadal variability in the mid-latitude subtropics of the North Pacific.

Key words: North Pacific, ventilated thermocline, regime shift, isopycnal model

1. Introduction

Decadal/interdecadal variations in the North Pacific have been investigated in many previous studies (Latif and Barnett, 1994; Deser et al., 1996; Zhang and Levitus, 1997; Gu and Philander, 1997; White and Cayan, 1998; Schneider et al., 1999; Minobe, 1999; Tourre et al., 1999, and references therein). Such a kind of phenomena was named as climate regime shift that carried out significant impacts on the physical and biological conditions in the North Pacific (Mantua et al., 1997). Besides the gyre-scale features associated with those changes in the North Pacific, a few basin-wide features relevant to interdecadal oceanic variability were found at the surface and subsurface (Zhang et al., 1998). Although the regime shift in the North Pacific had been investigated in previous studies, the exact scenario is not well understood yet, in particular, the subsurface in the North Pacific.

Simulation by forcing an oceanic general circulation model (GCM) is expected to evaluate these hypotheses of explanation derived from data analysis. However, most such studies have been done in the sense of idealization. For example, Liu and Shin (1999) forced a GCM by a patch of sea surface temperature (SST) anomalies in the central North Pacific. Nonaka and Xie (2000) used SST's interdecadal difference between 1977–1987 and 1965–1975 as a fixed anomalous heat flux. Lysne et al. (1997) reproduced the interdecadal variability by assimilating the surface and subsurface temperatures, however, the inherent physics in a GCM may be distorted somehow. In these previous works the spatial evolution, which implies an exact

*E-mail: dxwang@scsio.ac.cn

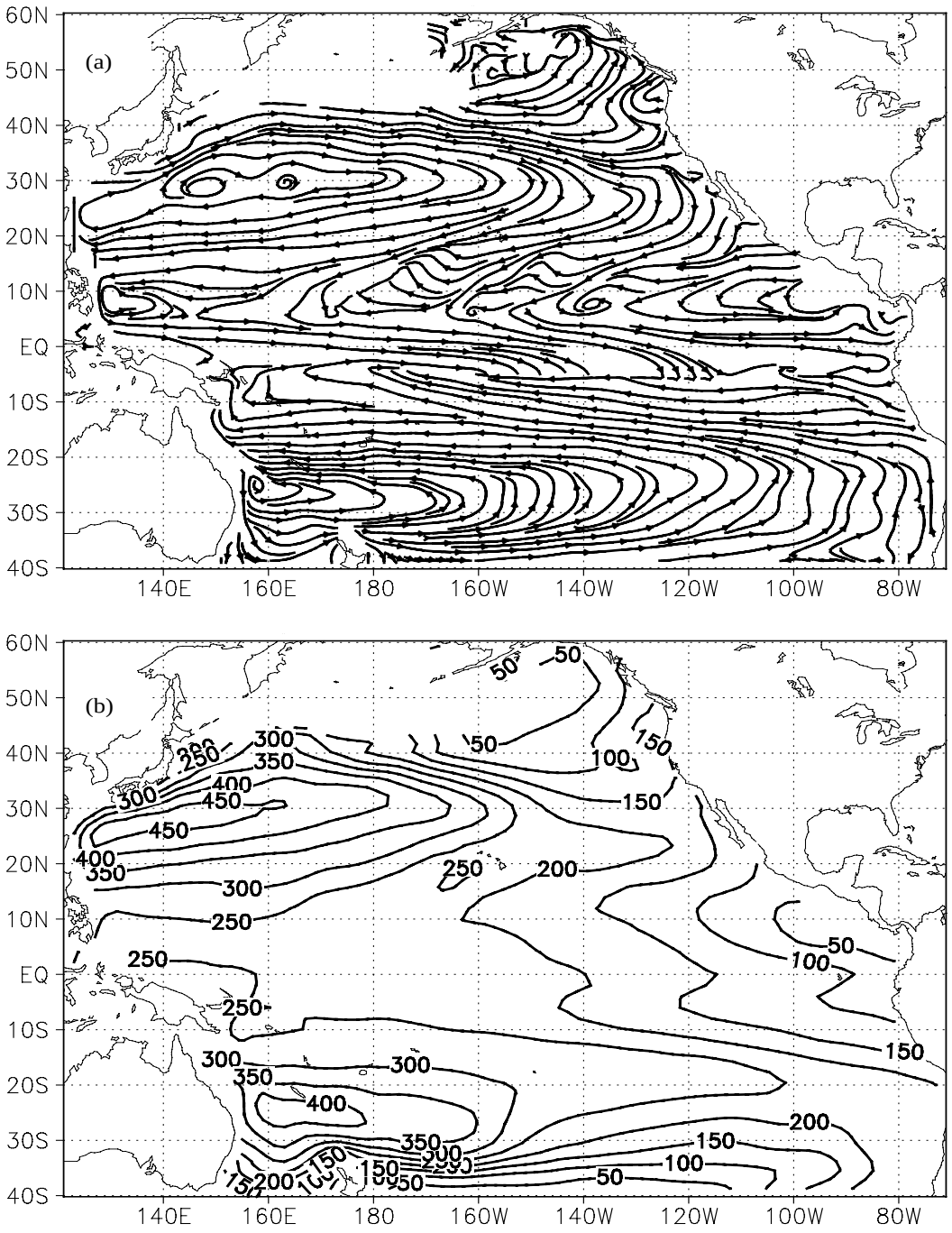

Fig. 1. January–February–March long-term mean of MICOM output over 1950–1993 at the sigma-26.0 layer. (a) stream pattern, (b) layer depth, units: m.

propagation of interdecadal signals with the basin scales, was not approached reasonably.

The present study extends the previous ones to a basin-wide issue by forcing an isopycnic layer model by the realistic, observed anomalies of SST and wind stresses. Our work focuses on the large-scale patterns of interdecadal variability in the North Pacific, with emphasis at the subsurface. The hypothesis that the thermal anomalies in the mid-latitude ocean propagate with subduction in the thermocline and reach the low-latitude ocean after several years, which had been proposed for the interdecadal oceanic variation by Deser et al. (1996), Zhang and Levitus (1997), Zhang and Liu (1999), and Schneider et al. (1999), is investigated

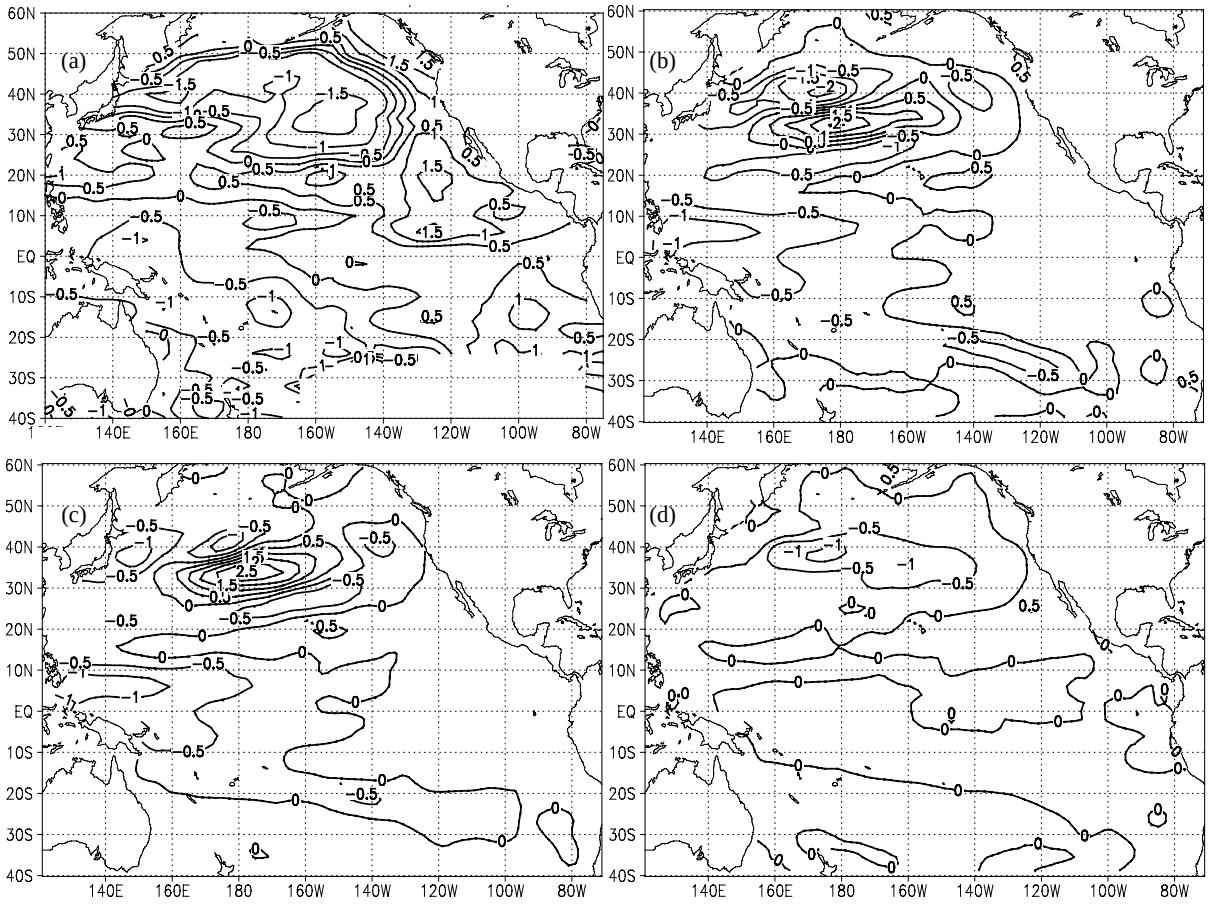

Fig. 2. Difference of HS400 between the pre- and post-1977 stages. (a) from XBT, (b) from Run A, (c) from Run B, (d) from Run C, contour interval is 0.5×10^9 W s m^{-2}.

through comparison with a theoretical framework of the ventilated thermocline. Three dimensional evolution of subducted thermal signals in the central North Pacific is simulated to speculate their pathway, traveling speed, penetrating process, and so on.

This paper is arranged as follows. In section 2, a brief introduction of an isopycnal ocean model and the experiment design are described. Section 3 focuses on the statistical comparison between observed and simulated variations regarding the potential basin-wide features. Section 4 investigates the 3-D structure of anomalies in the North Pacific. Then a summary and discussions appear in section 5.

2. Model, observations, and methods

The Miami Isopycnal Coordinate Ocean Model (known as MICOM, Bleck et al., 1992) is employed in the portion of the Pacific Ocean between 40°S and 60°N, very similar to the domains defined in previous numerical studies (Auad et al. 1999, Nonaka and Xie, 2000). The model consists of 15 isopycnal layers with full coupling to a bulk surface Kraus type mixed layer model (Kraus and Turner, 1967), which results in a reasonable resolution of thermocline. MICOM is forced with $2^\circ \times 2^\circ$ resolution, thus it has a roughly realistic coastline and bottom topography with the maximum depth at 5500 m. There are thermohaline fluxes across the southern end of the domain as a restoring term, whereas an enclosed momentum boundary condition is applied to all the lateral boundaries.

Surface forcing functions include monthly wind stresses and SST. All these data are from the Comprehensive Ocean Atmosphere Data Set (COADS) for 1945–1993 (Woodruff et al., 1987).

Generally, two methods can be used for heating the oceanic models. One is to drive the model with net heat fluxes; the other is to relax the surface temperature in the model to the observed one by a restoring scheme. The surface heating strategy we apply here

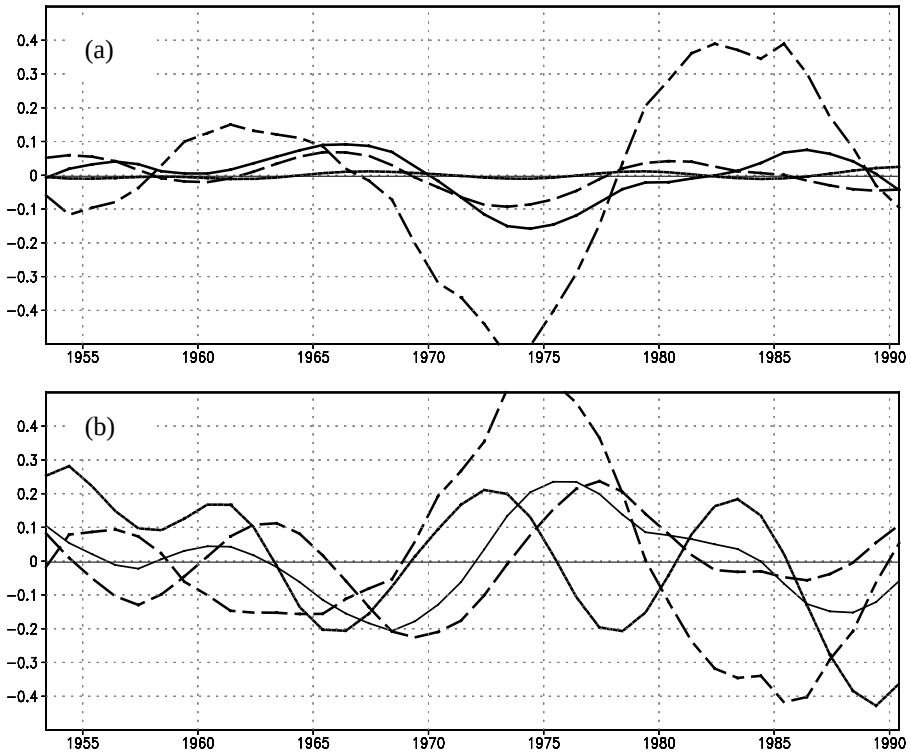

Fig. 3. Temporal evolution in reconstructed fields of the first CEOF mode for the simulated and observed HS400s. Long short dashed for the XBT's HS400, solid for Run A, long dashed for Run B, short dashed for Run C. (a) regional mean over 37.1°–53.8°N, 176°E–144°W, (b) region mean over 15.8°–48.8°N, 132°–120°W. Units in 10^9 W s m^{-2}.

adapts the relaxation condition, with a restoring time scale of 30 days.

Unless specificly mentioned, the model output data are summed up as a yearly mean for further analysis. A post-processing is done to provide the interannual signal with the variability removed by using a five-year running mean with uniform weights. As for the basin-wide characteristics, a complex EOF analysis (Barnett, 1983) is adopted to the heat storage of the upper 400 m layer (hereafter HS400), available in both the modeling and the eXpendable Bathy Thermograph (XBT) data (White, 1995).

Forced by monthly climatological wind stresses and SST derived from the COADS 40-yr dataset, MICOM is spun up for 50 years from a resting state with the Levitus temperature and salinity stratification. Three numerical experiments are designed to simulate the Pacific after the spinning-up. The control run (hereafter, Run A) is designed as driven by the COADS seasonal climatology of wind stresses and SST plus their anomalies from 1945 to 1993. Here we also name it as a full forcing run, i.e., forced by both the anomalous wind and heat fluxes. The long-term mean January-February-March fields over 1945–1993 are consistent with classic observations and GCM modeling in the Pacific Ocean (Fig. 1). For example, the stream pattern of sigma 26.0 in Run A shows a reasonable general circulation including the North Equatorial Current, North Equatorial Counter-Current, and the subtropical gyres. The long-term mean of the layer depth of sigma 26.0 matches very well to the observed results (Talley, 1985).

Two sensitivity runs are performed here. One concerns the wind forcing (hereafter, Run B) driven by the COADS climatology of wind stresses and SST plus wind stress anomalies during 1945–1993. The other is driven by the COADS climatology of wind stresses and SST plus SST anomalies for 1945–1993 (hereafter, Run C).

3. Comparison of modeled and observed evolutions

According to the previous studies, the pre- and post-1977 stages are defined regarding the SST abnormal shift from warm to cold in the central North Pacific (Minobe, 1999). The pre-1977 stage refers to the ten-year mean over 1968–1977 while the post-1977 stage the successive ten-year mean over 1978–1987.

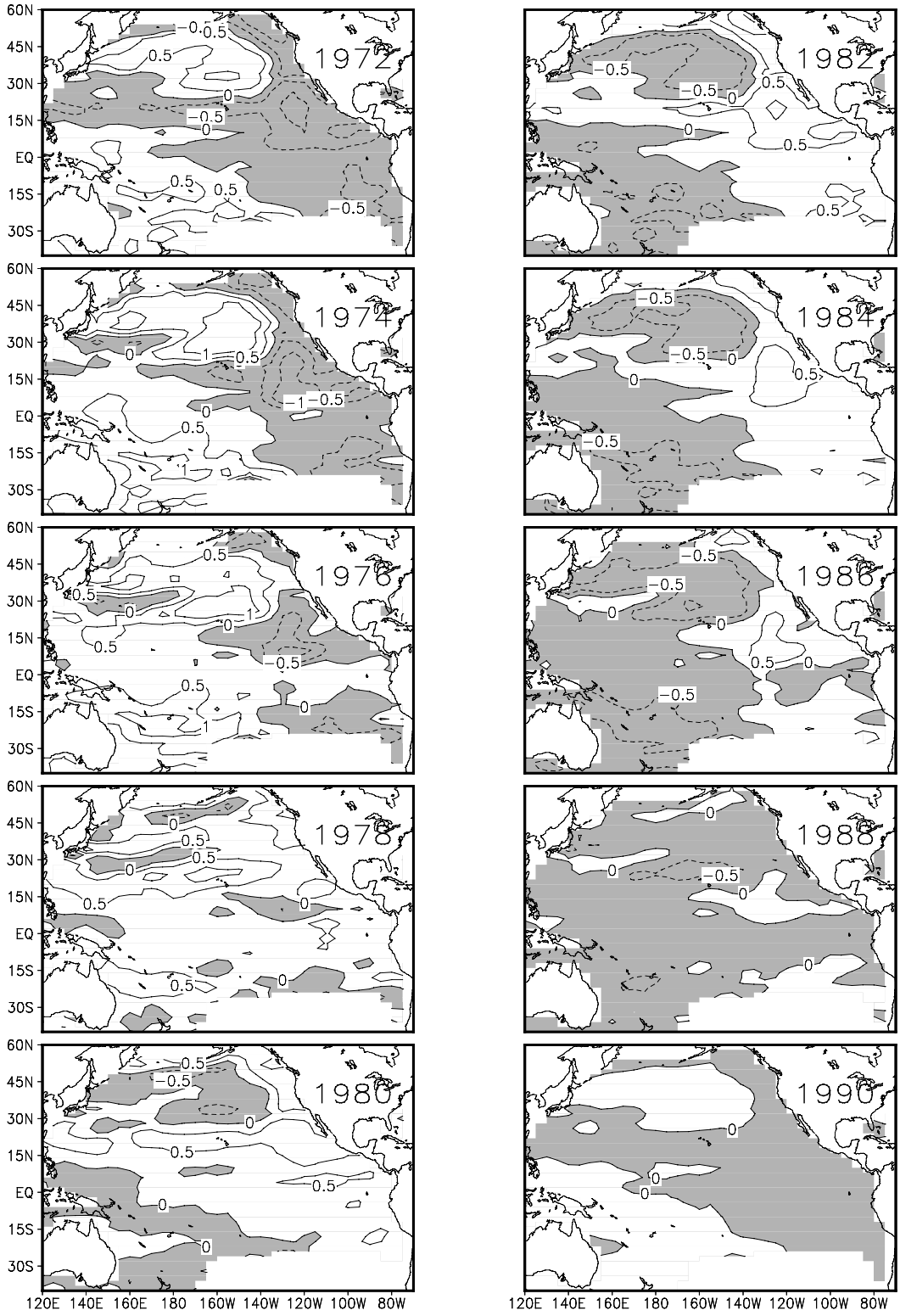

Fig. 4. 1972–1990 biyearly evolution in the original HS400 after five-year running mean. The first ten panels are from XBT data and the others are from Run C. Shaded area is negative, contour interval is 0.5×10^9 W s m^{-2}.

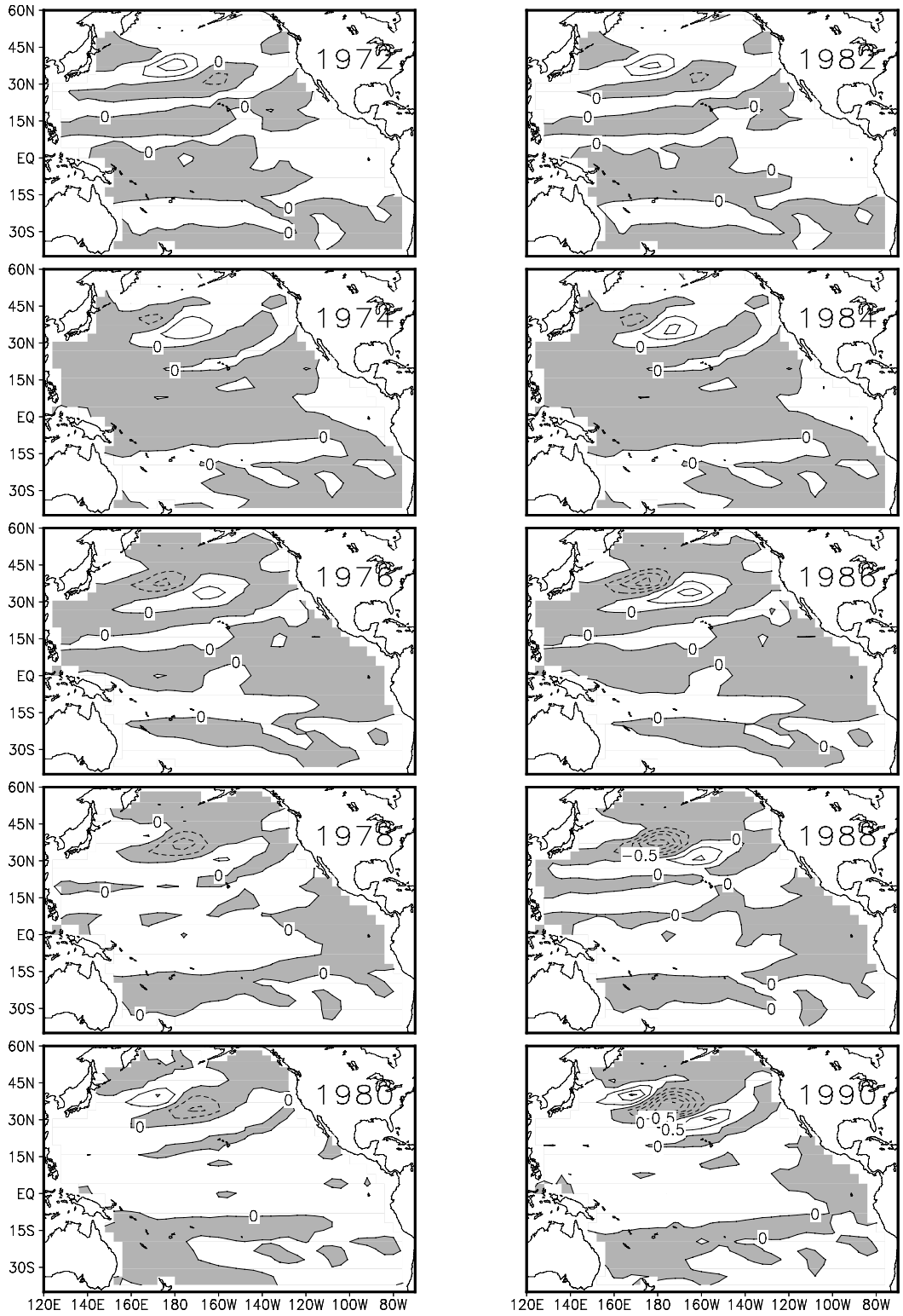

Fig. 4. (Continued)

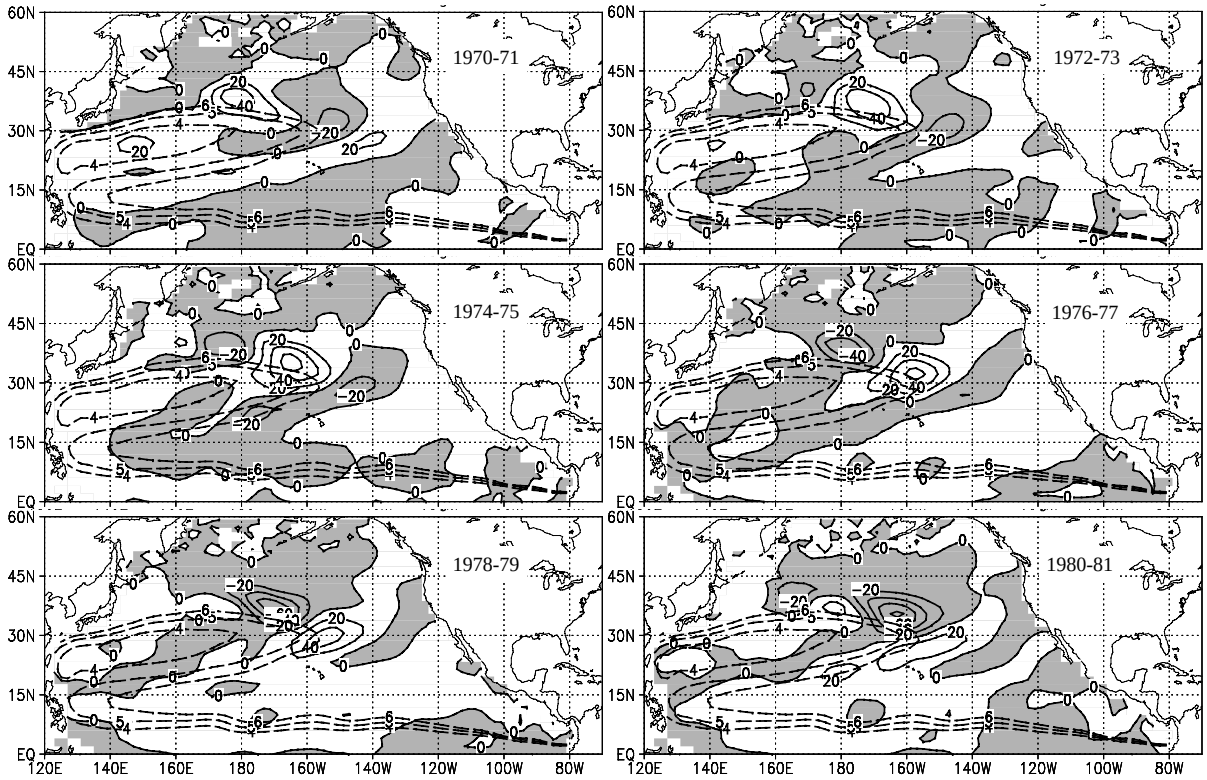

Fig. 5. Biyearly mean of thickness anomalies between sigma 24.5 to 26.0 from Run C five-year running mean output in the North Pacific. Shaded area is negative, contour interval is 20 m. Heavy dashed contours superposed indicate three potential vorticity lines, 4×10^{-10}, 5×10^{-10}, 6×10^{-10} m^{-1} s^{-1}, respectively.

The observed interdecadal variations of SST, wind stresses, and the heat storage of the upper 400m layer are synchronized with one another, especially in the four regions with significance (Wang et al. 2003). They are the central North Pacific, the central subtropical Southern Pacific, the Gulf of Alaska, and the central and eastern tropical Pacific with different signs. HS400 anomalies from XBT in the former two regions are in phase, so in the latter two regions, whereas the former's and the latter's are out of phase. The modeled HS400 provides this relationship in terms of the interdecadal jump (Fig. 2).

In addition to this feature, it should be noted that in the central North Pacific and Gulf of Alaska, the locations of the significant signatures of SST, HS400, and zonal wind stresses are almost the same (Wang et al., 2003). So also the signatures in the southern subtropical Pacific Oceans. Such correspondence with each other strongly suggests that the major portion of the interdecadal variation may be partly driven by local factors except in the tropics. In other words, the local air-sea feedback also plays an important role in the interdecadal variability away from the equator, besides a possible internal connection driving the local signals to other regions.

The off-equatorial feature for interdecadal signals in the simulated HS400 in the eastern tropical Pacific matches the XBT observations very well. Note that the simulated strength of these anomalies is comparable to the observations with the exception that the signal in the eastern subtropical Pacific is underestimated and it is overestimated in the western tropical Pacific. Another shortcoming in simulation is that the zonal band of positive interdecadal signals, observed in 20°–30°N, now shifts northward by about 5 degrees.

The interdecadal differences of HS400 between the pre- and post-1977 stages simulated by Run A, Run B, and Run C do not demonstrate exactly the same patterns associated with the regime shift in the late 1970s (Figs. 2 and 3). The interdecadal signals in the North Pacific in Run B are identical to those in Run A. However, compared to the observations, the positive interdecadal signals of HS400 in the central North Pacific generated in Run B are weaker than those in Run A, and the zonal band with a positive signature around 20°N occurs, since the negative signal of the west part of the zonal band in Run A is reversed compared to Run B.

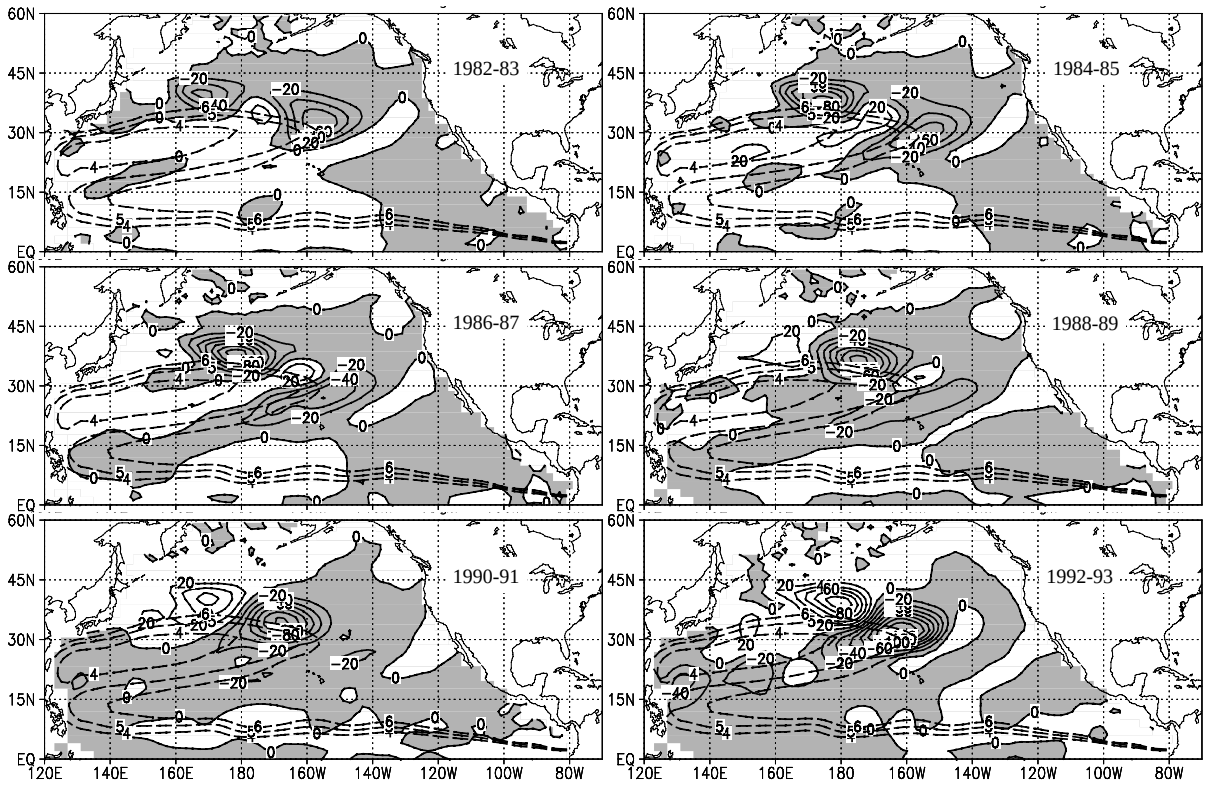

Fig. 5. (Continued)

Concerning the shape of the simulated signature in the central North Pacific, there is a core with opposite sign to the surroundings, which is injected into the oval shape of the HS400 anomalies in Run A and Run B. But such a core disappears in Run C. Therefore, the oval-shaped anomalies are formed with much agreement with the observed ones in Run C (Fig. 2d).

Improvement is also great in Run C regarding the interdecadal signals in the subtropical North Pacific. As in the discussion about the control run in section 3, overestimation of the interdecadal signals can be seen in the western and central subtropical Pacific, whereas, underestimation occurs in the eastern subtropical Pacific and the Gulf of Alaska. There exists such a disagreement in Run B too. However, such a disagreement with observation is greatly reduced in the simulation by Run C. For example, the zonal band around 20° with positive interdecadal signals occurs again, just like the observed one. From the basin-wide feature comparison, at least based on characteristics of the first CEOF mode, we speculate that the pattern and evolution are in remarkably good agreement with the observation in view of the interdecadal variability in the three experiments. Due to enhanced modeling in the mid-latitudes and subtropics, the interdecadal transition in the North Pacific will be analyzed utilizing the model output from Run C in the next section.

The first complex EOF modes for both the simulated and observed HS400 are compared based on their temporal evolution and spatial structures. The first mode of the observed HS400 explains 43.5% of the total variance while that of the simulated HS400 is 34.0%. From the spatial fields of amplitude for both HS400's simulation and observation, it is shown that there are large amplitudes in the North Pacific and the subtropics (figures not shown), consistent with the interdecadal difference between the pre- and post-1977 stages.

Comparison of the temporal phases for the simulated and observed regime shift in the 1970s reveals that there is a two-year lag in the simulation in view of the basin-wide HS400 features with interdecadal timescales (Fig. 3). When a period of about 20 years for the interdecadal variability is concerned, such a phase lag is acceptable, justified from the well-matching spatial features.

4. Subsurface transition in the North Pacific

Improved modeling in Run C for the signals in the

North Pacific motivates the following analysis through which the simulated interdecadal variability forced by pure buoyancy fluxes is investigated. Such analysis will demonstrate the agreement between the modeling dynamics and theoretical results from the ventilated thermocline in the mid-latitudes and subtropics.

Possible propagation in the North Pacific provided by the bi-yearly mean diagrams of the observed HS400 anomalies is described as follows (Fig. 4). Starting from the central North Pacific (about 30°–40°N, 170°–140°W), the interdecadal signals propagate southwestward until reaching about 16°N. Another propagation in an opposite direction happens for the interdecadal signals in the western tropical Pacific. These two kinds of signals merge near 16°N latitude. Actually, there is a band which is an important indicator since it acts as a buffer layer where two pieces of propagation with opposite directions come to merge gradually (Wang and Liu, 2000). In the tropics, there is a prominent propagation from west to east for the interdecadal variability of HS400.

There is significant difference in the propagating tendency between the interdecadal signals in the observed SST and HS400. Generally, the SST's interdecadal signals are stationary from complex EOF analysis (figure not shown). Therefore, there is a sharp out-of-phase relationship between SSTs in the central North Pacific and in the tropics. Nevertheless, the HS400's interdecadal signals in these regions hold a sense of propagation. In the tropics, the interdecadal variation of SST is uniformly in phase, except in the far western Pacific. In contrast with SST, the spatial phase field of HS400 from the complex EOF analysis leads to a clear delineation of eastward propagation in the tropical Pacific.

This suggests there are different physics responsible for the interdecadal variability at the surface and the subsurface or thermocline, although the basin-wide evolutions for SST and HS400 are almost simultaneous on the interdecadal timescales. MICOM can generate a clear basin-wide evolution like the observations, which consists of several kinds of propagation in the central North Pacific, the subtropical western Pacific, and the tropics, although there is no propagation in the surface forcing functions, e.g., SST and wind stresses.

Schneider et al. (1999) clarified that the observed anomalies follow a path around the edge of a potential vorticity pool in the western subtropical Pacific. It should be addressed that the downward and southwestward migration of those temperature anomalies in the simulation is consistent with the scenario of the ventilated thermocline and its resulting subduction in the central North Pacific.

Both the horizontal patterns of thickness anomalies and vertical section snapshots of temperature anomalies in this simulation strongly support these observed processes (Figs. 5 and 6). The simulated temperature anomalies in the vertical-meridional section at 170°–145°W propagate along a certain isopycnal layer after the anomalies detrain from the mixed layer in the subduction region of the central North Pacific. It takes about 8–10 years for the signatures in the central North Pacific to propagate from 35°N to 25°N. That means, no matter how these temperature anomalies are originally excited by Ekman pumping relevant to anomalous wind forcing, or by buoyancy forcing associated to anomalous heat fluxes, propagation is identified as adiabatic thermocline adjustment. No further southward propagation in Fig. 6 is due to the section departing the edge of a potential vorticity pool south to 20°N (Fig. 5).

There is an oval-shaped pattern of anomalies formed in the central North Pacific (Fig. 1), especially at the subsurface. The oval-shaped pattern of anomalies becomes more dominant in the observed temperature fields with depth increase (figure not shown). In an idealized layered model, such a kind of oval-shaped pattern of anomalies is also pronounced at the subsurface layer around the ventilated thermocline (Huang and Pedlosky, 1999). So does GCM modeling (Nonaka and Xie, 2000). This shape is formed exactly due to certain internal oceanic processes. At least two factors modulate the thermal anomalies in the central North Pacific. One is the advected subduction, which pulls the anomalies southward loaded by the interior Sverdrup currents. The other is westward propagation of the baroclinic Rossby wave in the mid-latitudes, which pushes the anomalies westward. Given a bowl shape of SST anomalies, as a result, the signal is distorted into an oval-like shape at the subsurface.

Here we use the potential vorticity fields to highlight how much the theory of ventilated thermoclines works for the interdecadal signals in the North Pacific. Potential vorticity is obtained from the following under the limit of small Rossby number and in a layered fluid remarked by density profiles simulated by MICOM.

$$q = (f\triangle\rho)/(\rho_0\triangle H) \ ,$$

where f is the Coriolis parameter, $\triangle H$ is the isopycnic layer thickness, ρ_0 is the reference density, and $\triangle\rho$ is the density jump between the upper and lower interfaces of that isopycnic layer.

The thickness anomalies with sigma 24.5 to 26.0 simulated by MICOM show that it seems the advected subduction prevails during the spatial evolution of the

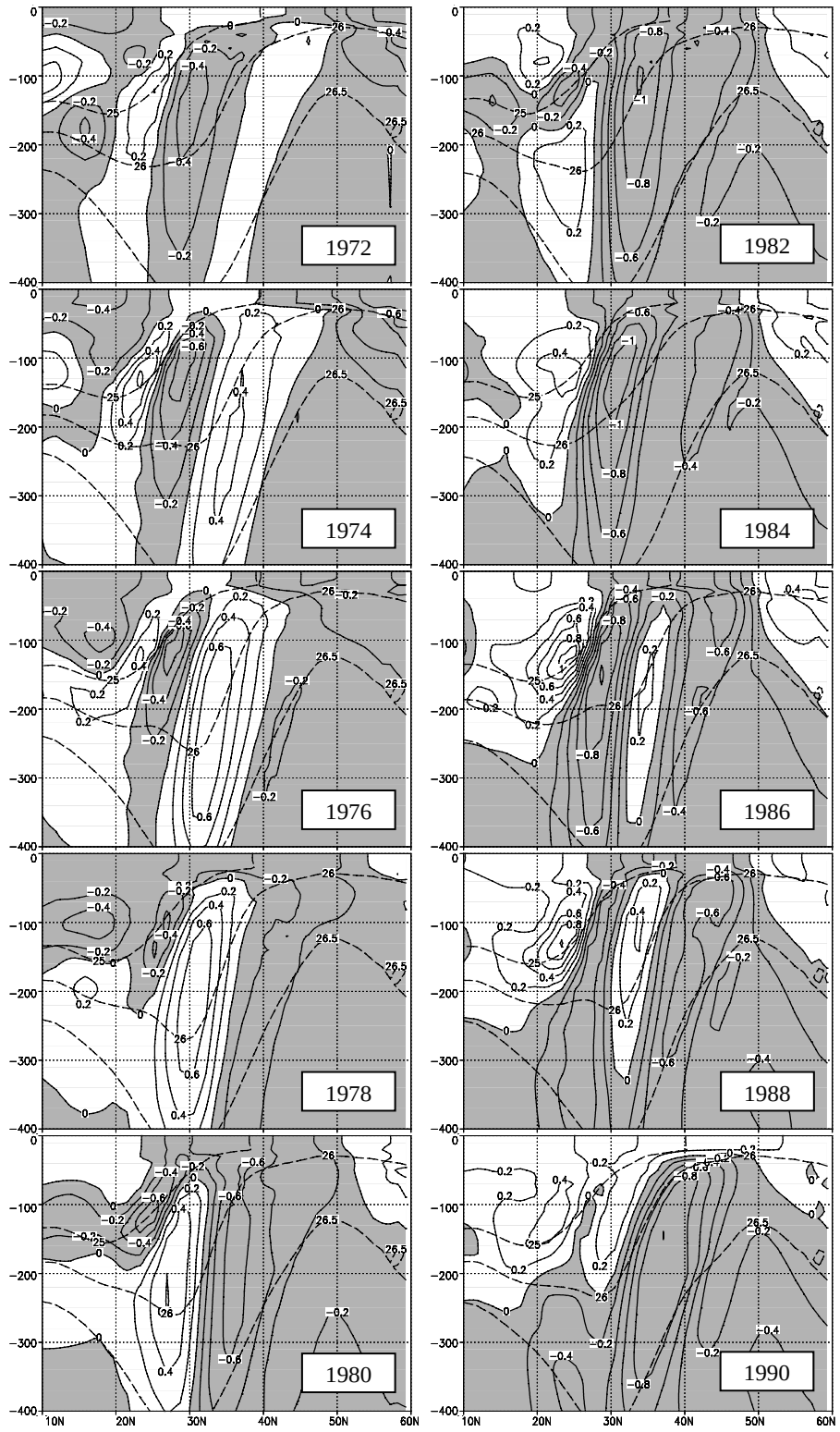

Fig. 6. Temperature anomalies at the vertical section averaged over 175°–145°W from Run C five-year running mean output in the North Pacific. Contour for temperature is 0.2°C. Long dashed contours superposed indicate the density profile at the same section, which was defined during the same period. From upper to lower, sigma is 25, 26, 26.5, respectively.

interdecadal signals in the North Pacific, since the signals move exactly along a path with constant potential vorticity (see Figs. 5a and 5b). In other words, both warm and cold signals take a track as the edge of the potential vorticity pool exists within the subtropical gyre. An explanation proposed by Liu and Shin (1999) and Nonaka and Xie (2000) says active tracers like temperature anomaly will take a more southwestward way rather than a purely westward path taken by a passive tracer. This suggests that although the baroclinic Rossby waves may favor the vertical mode of temperature anomalies in the simulation, temperature anomalies mostly follow the physics of the ventilated thermocline due to their active feature. Another piece of proof for the active thermodynamics is that those temperature anomalies tend to decline when propagating southwestward.

5. Discussions and summary

An isopycnal coordinate ocean model is driven with the observed monthly COADS wind stresses and SST in the present study. The simulation over 1945–1993 shows a robust interdecadal variability in the different dynamic regions such as the central North Pacific, the Gulf of Alaska and the eastern subtropical Pacific, and the western tropics and the southern subtropics. The basin-wide evolution of the interdecadal signals both temporally and spatially matches the observed characteristics very well in view of a statistical analysis. However, the shortcoming of these simulations still exists, for example, there are several instances of underestimation or overestimation in certain regions, while a lag of two years appeared in the simulation evolution when compared to the observation.

The scenario for the thermal anomalies on the equatorward side of 16°N is manifested as propagation with opposite direction associated with those anomalies on the polarward side of 16°N, just as in the observation analysis conducted by Wang and Liu (2000). Before 1972, when a warm signal is formed in the subduction region in the central North Pacific, another warm signal is already being stimulated in the western tropical Pacific. This warm signal will move northeastward also along a path with constant potential vorticity. The anomalies on the polarward side of 16°N take a similar path actually. There are different forcing mechanisms for those signals loaded by downstream and upstream migration since they are excited in different dynamic regions. Southwestward motion in the subtropics is driven remotely by anomalous buoyancy forcing in the central North Pacific because Run C improves the agreement with observation. However, northeastward propagation in the western tropical Pacific is generated locally by anomalous wind forcing since signal strength and its propagation are reduced when the tropical wind forcing is turned off.

In the present simulation and observation analysis, there is no distinct evidence for a single-direction connection between subsurface temperature anomalies in the mid-latitude North Pacific and the tropics through which subsurface anomalies can penetrate through the subtropics into the tropics. What Zhang et al. (1998) revealed using Levitus data did not appear here. The enhanced positive HS400 anomalies in the western tropical Pacific since the 1970s, which were regarded as results of penetration from the mid-latitudes and responsible for increasing the intensity of the ocean-atmosphere interaction in the tropics, should be reconsidered. There must be other processes which favor warm interdecadal signals in the western tropical Pacific, since such signals were not actually formed later than those in the central North Pacific.

In our simulation results, the interior subsurface signals generated by a ventilated thermocline in MICOM are consistent with the XBT observation regarding their source, pathway, and traveling speed, however, further investigation is needed. These important findings are intrinsic to further study of the predictability of the interior oceans on the interdecadal timescales.

Acknowledgments. The authors are grateful to Drs. Shi Ping, S.-I. Shin, and Chang Ping for their helpful discussions. This study was supported by the IARC-Frontier Research System for Global Change, the National Natural Science Foundation of China (40136010) and the Chinese Academy of Sciences (KZCX2-205 and KZCX2-203).

REFERENCES

Auad G., Miller, A. J. White, W. B., 1998: Simulation of heat storages and associated heat budgets in the Pacific Ocean, 2, Interdecadal timescale. *J. Geophys. Res.*, **103**, 27621–27635.

Barnett, T. P., 1983, Interaction of the monsoon and Pacific trade wind system at interannual time scales. Part I: The equatorial zone. *Mon. Wea. Rev.*, **111**, 756–773.

Bleck, R., C. Rooth, D. Hu, and L. T. Smith, 1992: Salinity-driven transients in a wind- and thermohaline-forced isopycnic coordinate model of the North Atlantic. *J. Phys. Oceanogr.*, **22**, 1486–1505.

Deser, C., M. A. Alexander, and M. S. Timlin, 1996: Upper-ocean thermal variations in the North Pacific during 1970–1991. *J. Climate*, **9**, 1840–1855.

Gu, D. F., and S. G. H. Philander, 1997: Interdecadal climate fluctuations that depend on exchanges between the tropics and extratropics. *Science*, **275**, 805–807.

Huang, R. X., and J. Pedlosky, 1999: Climate variability inferred from a layered model of the ventilated thermocline. *J. Phys. Oceanogr.*, **29**, 779–790.

Kraus, E. B., and J. S. Turner, 1967: A one-dimensional model of the seasonal thermocline, II The general theory and its consequences. *Tellus*, **19**, 98–105.

Latif, M., and T. P. Barnett, 1994: Causes of decadal climate variability over the North Pacific and North America. *Science*, **266**, 634–637.

Liu, Z., and S.-I. Shin, 1999: On thermocline ventilation of active and passive tracers. *Geophys. Res. Lett.*, **26**, 357–360.

Lysne, J., P. Chang, and B. Giese, 1997: Impact of the extratropical Pacific on equatorial variability, *Geophys. Res. Lett.*, **24**, 2589–2592.

Mantua, N. J., S. R. Hare, Y. Zhang, J. M. Wallace, and R. C. Francis, 1997: A Pacific interdecadal climate oscillation with impacts on salmon production. *Bull. Amer. Meteor. Soc.*, **78**, 1069–1079.

Minobe, S., 1999: Resonance in bidecadal and pentadecadal climate oscillations over the North Pacific: role in climatic regime shifts. *Geophys. Res. Lett.*, **26**, 855–858.

Nonaka, M., and S.-P. Xie, 2000: Propagation of North Pacific interdecadal subsurface temperature anomalies in an ocean GCM. *Geophys. Res. Lett.*, **27**, 3747–3750.

Schneider, N., A. J. Miller, M. A. Alexander, and C. Deser, 1999: Subduction of decadal North Pacific temperature anomalies: Observations and dynamics. *J. Phys. Oceanogr.*, **29**, 1056–1070.

Talley, L. D., 1985: Ventilation of the subtropical North Pacific. *J. Phys. Oceanogr.*, **15**, 633–649.

Tourre, Y. M., Y. Kushnir, and W. B. White, 1999: Evolution of interdecadal variability in sea level pressure, sea surface temperature and upper ocean temperature over the Pacific Ocean. *J. Phys. Oceanogr.*, **29**, 1528–1541.

Wang Dongxiao, and Zhengyu Liu, 2000: The pathway of the interdecadal variability in the Pacific Ocean. *Chinese Science Bulletin*, **45**(17), 1555–1561.

Wang Dongxiao, Wang Jia, Lixin Wu, and Zhengyu Liu, 2003: Relative importance of wind and buoyancy forcing for interdecadal regime shift in the Pacific Ocean. *Science in China, D*, **46**(5), 417–427.

White, W. B., 1995: Design of a global observing system for gyre-scale upper ocean temperature variability. *Progress in Oceanography*, **36**, 169–217.

White, W. B., and D. R. Cayan, 1998: Quasi-periodicity and global symmetries in interdecadal upper ocean temperature variability. *J. Geophys. Res.*, **103**, 21335–21354.

Woodruff, S. D., R. J. Slutz, R. L. Jenne, and P. M. Steurer, 1987: A comprehensive ocean-atmospheric data set. *Bull. Amer. Meteor. Soc.*, **68**, 1239–1250.

Zhang, R.-H., and S. Levitus, 1997: Structure and cycle of decadal variability of upper ocean temperature in the North Pacific. *J. Climate*, **10**, 710–727.

Zhang, R.-H., L. M. Rothstein, and A. J. Busalacchi, 1998: Origin of upper-ocean warming and El Niño changes on decadal scales in the tropical Pacific Ocean. *Nature*, **391**, 879–883.

Zhang, R.-H., and Z. Liu, 1999: Decadal thermocline variability in the North Pacific Ocean: Two pathways around the subtropical gyre. *J. Climate*, **12**(11), 3273–3296.